Adv. Exp. Med. Biol. 543: 39-55 (2003)

Chapter 3

OXYGEN CONFORMANCE OF CELLULAR RESPIRATION

A perspective of mitochondrial physiology

Erich Gnaiger

Abstract: Oxygen pressure declines from normoxic air-level to the microenvironment of mitochondria where cytochrome *c* oxidase (COX) reduces oxygen to water at oxygen levels as low as 0.3 kPa (2 Torr; 3 μM; 1.5 % air saturation). Intracellular hypoxia is defined as (1) local oxygen pressure below normoxic reference states, or (2) limitation of mitochondrial respiration by oxygen levels below kinetic saturation, resulting in oxyconformance. High-resolution respirometry provides the methodology to measure mitochondrial and cellular oxygen kinetics in the relevant low oxygen range <1 kPa (7.5 mmHg; 9-10 μM; 5 % air saturation). Respiration of isolated heart mitochondria follows hyperbolic oxygen kinetics with half-saturating oxygen pressure, p_{50}, of 0.04 kPa (0.3 Torr; 0.4 μM) in ADP-stimulated state 3. Thus mitochondrial respiration proceeds at 90 % of its hyperbolic maximum at the p_{50} of myoglobin, suggesting the possibility of a small but significant oxygen limitation even under normoxia in active muscle. Any impairment of oxygen delivery, therefore, induces oxyconformance. In addition, a shift of mitochondrial oxygen kinetics to the right, particularly by competitive inhibition of COX by NO, causes a further depression of respiration and a compensatory increase of local oxygen pressure. Above 1 kPa, mitochondrial oxygen uptake increases above hyperbolic saturation, which is probably due to oxygen radical production rather than the kinetics of COX. In cultured cells, the pronounced oxygen uptake above mitochondrial saturation at air-level oxygen pressure cannot be inhibited by rotenone and antimycin A, amounting to >20 % of routine respiration in fibroblasts. Biochemical models of oxyconformance of COX are evaluated relative to patterns of intracellular oxygen distribution in the tissue and enzyme turnover in vivo, considering the kinetic effects of COX excess capacity on flux through the mitochondrial electron transport chain.

Key Words: oxygen kinetics, cytochrome *c* oxidase, mitochondrial respiratory control, oxygen limitation, hypoxia

Hypoxia: Through the Lifecycle, edited by R.C. Roach *et al.*
Kluwer Academic/Plenum Publishers, New York, 2003.

INTRODUCTION

The high affinity of cytochrome *c* oxidase for oxygen implies independence of mitochondrial respiration of oxygen over a wide range of oxygen levels, which gives rise to the paradigm of "oxygen regulation", although "kinetic oxygen saturation" describes more accurately the underlying mechanism. In contrast, various degrees of oxyconformance are observed in cells (2, 9, 28, 33, 36). Biochemical and physiological approaches are required to separate the primary kinetic mechanisms from secondary effects of oxygen sensing, signalling, gene expression and protein synthesis or degradation. Modern trends in mitochondrial bioenergetics integrate *(1)* molecular and enzyme kinetic properties of the membrane proteins constituting the electron transport chain, particularly the proton pumps such as cytochrome *c* oxidase (70), *(2)* synkinetic properties of the mitochondrial metabolic network involved in the control of flux and energetic efficiency (26, 27), and *(3)* the regulatory role of mitochondrial signalling in the cell and of intracellular conditions in the tissue. From such studies concepts emerged on reactive oxygen species (ROS) signalling cascades (37, 44), redox signalling (34), the protective role of regulated low intracellular pO_2 (22, 27, 58), and the mitochondria-dependent pathway of controlled cell death or apoptosis (4).

Approaching the problem of hypoxia and oxygen dependence of respiration from such a perspective of mitochondrial physiology, this review *(1)* relates classical enzyme kinetics of cytochrome c oxidase with mitochondrial respiratory control, *(2)* contrasts mitochondrial oxygen kinetics and oxygen dependence of cellular respiration, *(3)* illustrates the importance of oxygen diffusion in determining oxygen conformance of respiration in various cell types and tissue preparations, and *(4)* discusses concepts on the energetics of metabolic downregulation under hypoxia in the light of these baseline studies.

HYPOXIA OR HYPEROXIA IN ISOLATED AND CULTURED CELLS

Several apparent paradoxes have emerged in the physiology and pathology of hypoxia, such as the oxygen, lactate, efficiency, and diving paradoxes (32). While some have been rationalized and solved, others remain hot spots of current research. Another apparent paradox on hypoxia arises in studies of the bioenergetics of isolated and cultured cells, where respiration, contractile performance or protein synthesis are apparently oxygen limited at partial pressures at or above normoxic tissue levels. Such extended oxygen conformance deviates from the "regulatory" pattern or oxygen independence of mitochondrial respiration to <1 kPa (7.5 mmHg (28)). Respiration of various chronically or acutely exposed cell types is partially oxygen dependent up to >50 % air saturation (2, 33, 54, 61). The response pattern is biphasic and corresponds to microxic regulation, characterized by a steep increase of flux at low oxygen and a more shallow oxyconformance at high oxygen levels (21).

Compared with ambient oxygen pressure of 20 kPa (150 mmHg), oxygen levels are low within active tissues and are under tight control by microcirculatory adjustments to match oxygen supply and demand. Alveolar normoxia of 13 kPa (100 mmHg) contrasts

with a corresponding 1 to 5 kPa (10 to 40 mmHg) extracellular pO_2 in solid organs such as heart, brain, kidney and liver (19). Considering the respiratory cascade and oxygen in the microenvironment of tissue (23, 26), it appears surprising that protein synthesis becomes inhibited in hepatocytes incubated at a "hypoxic" pO_2 of 11 kPa (80 mmHg) compared with 95 % oxygen (41), hepatocyte respiration is reduced at 9 kPa (70 mmHg (54)), and cytochrome *c* oxidase is reversibly inhibited at 50 μM (4 kPa or 30 mmHg (16)). Does this suggest substantial oxygen limitation of aerobic ATP production and protein synthesis to prevail under normoxia *in vivo*, or are responses to oxygen altered *in vitro*?

Protein synthesis in isolated cardiomyocytes is inhibited at 0.05 kPa (0.4 mmHg) but not at 0.5 kPa. Casey et al. (12), therefore, suggest that part of the apparent oxygen paradox may be due to oxygen gradients giving rise to differences between the gas phase and the cell level. Pericellular pO_2 falls to <0.03 kPa (0.2 mmHg) in human hepatoma cells growing in monolayer culture with 95 % air in the gas phase, when respiration is significantly oxygen limited (43). Continuous cultures of mouse hybridoma cells grow with optimum yield at 0.5 % air saturation (0.5 kPa; 4 mmHg; (45)), and the biochemical efficiency of ATP production per oxygen consumed is high in isolated mitochondria under severely limiting hypoxia at pO_2 as low as 0.002 kPa (0.014 mmHg; (27)). Advancements in the study of mitochondrial and cellular oxygen kinetics may help to clarify some controversial aspects of respiratory control under hypoxia.

HIGH-RESOLUTION RESPIROMETRY AT LOW LEVELS OF OXYGEN

Our studies on the oxygen dependence of mitochondrial (Figs. 1 and 2), cellular (Figs. 3 and 4) and tissue respiration (Figure 6) are based on high-resolution respirometry with the twin-chamber Oroboros® *Oxygraph* with chamber volumes set at 2 ml. The software *DatLab* (Oroboros, Innsbruck, Austria) is used for data acquisition (1 or 2 s time intervals) and analysis, including calculation of the time derivative of oxygen concentration to obtain a continuous on-line record of flux, signal deconvolution dependent on the response time of the oxygen sensor, and oxygen-dependent correction for instrumental and chemical background oxygen flux. Oxygen back-diffusion at low oxygen is minimized in this system by the use of gas-impermeable materials, with glass chambers, titanium stoppers, PEEK-coated magnetic stirrer bars, viton O-rings and butyl rubber sealings. High signal stability and dynamic background correction for oxygen consumption of the oxygen sensor and oxygen backdiffusion provide the basis for high resolution of oxygen flux (<2 $pmol.s^{-1}.cm^{-3}$). Signal noise decreases with decreasing oxygen to less than ±0.003 kPa (0.02 mmHg; recorded near zero oxygen over 100 data points and 1 s intervals), which is of particular advantage for studies in the range of physiological intracellular oxygen levels and hypoxia. A dynamic correction for sensor drift at zero oxygen pressure extends the sensitivity to this low noise level. Instrumental design, experimental procedures and data analysis are described in detail elsewhere (22, 28, 61).

EXCESS CAPACITY OF CYTOCHROME *C* OXIDASE AND RESPIRATORY FLUX CONTROL

The terminal acceptor for oxygen of the mitochondrial electron transport chain, cytochrome *c* oxidase (COX), has the capacity to operate at a turnover rate of 300 electrons per second when studied as an isolated enzyme (49). When the enzyme remains integrated in the inner membrane of isolated mitochondria, however, the turnover rate is about 6-fold less. This is the case when complex IV of the respiratory chain (COX) is studied as an isolated step, by blocking complex III with antimycin A and feeding electrons from the artificial substrate TMPD to cytochrome *c* and COX (Figure 1). Under these conditions, electron flux is coupled to proton translocation and is stimulated by ADP. The reaction velocity depends further on the concentration of reduced TMPD (500 µM in our studies), which is held constant by an excess concentration of ascorbate (2 mM; Figure 1). In heart mitochondria, even this COX turnover rate is twice above the maximum physiological value, which is measured as oxygen flux through the entire respiratory chain with the physiological substrates pyruvate and malate (Figure 1).

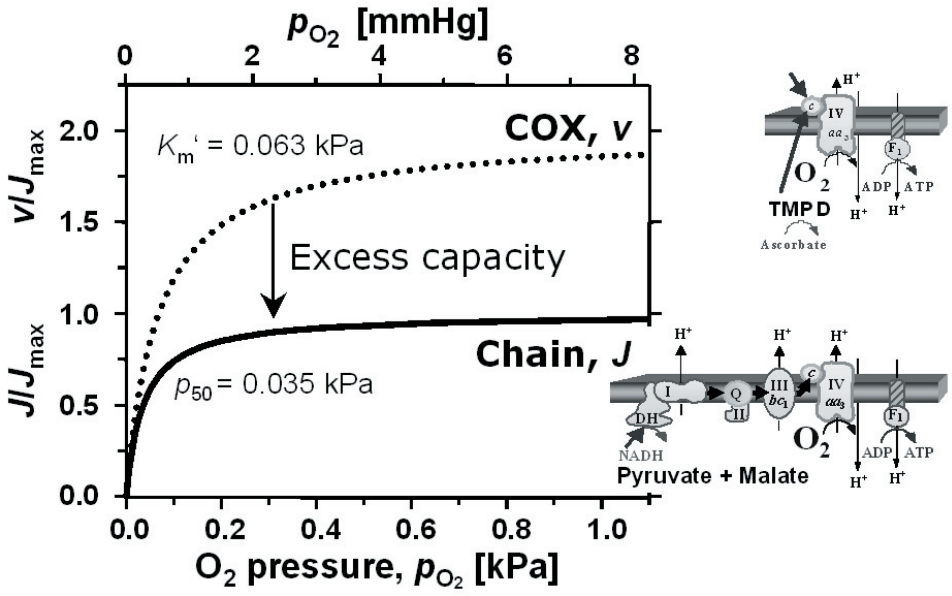

Figure 1. Oxygen kinetics in isolated heart mitochondria for reaction velocity, *v*, of the isolated step of complex IV (cytochrome *c* oxidase, COX (23)) and for oxygen flux, *J*, through the respiratory chain (25). Coupled respiration was stimulated to state 3 by ADP. Maximum reaction velocity of COX with 0.5 mM TMPD, 2 mM ascorbate and 2.5 µM antimycin A was about two times higher than respiratory flux with 5 mM pyruvate and 2 mM malate. Proportional to COX turnover, the apparent half-saturation constant, K_m', was about two times higher for COX (0.47 mmHg) than the p_{50} for the respiratory chain (0.26 mmHg). The oxygen range for kinetic analysis corresponds to 10 µM O_2 or 5 % air saturation.

The oxygen kinetics of cytochrome *c* oxidase in mitochondria follows a monophasic hyperbolic function over an oxygen concentration range >10 times the apparent half-saturation or Michaelis-Menten constant, K_m'. The K_m' of COX in rat heart mitochondria is 0.67 ± 0.12 μM (23), equivalent to 0.063 kPa or 0.47 mmHg (Figure 1). The K_m' is not a constant but depends on enzyme turnover (69), hence the physiological p_{50} of mitochondrial respiration is even lower at 0.035 kPa or 0.26 mmHg at maximum activity (state 3; Figure 1). The p_{50} is further attenuated at submaximal activity, dropping off to 0.014 kPa or 0.1 mmHg in the resting state of ADP-limited respiration (26). These values illustrate the specific demand imposed on high-resolution respirometry for accurately measuring and maintaining low levels of dissolved oxygen in suspensions of isolated mitochondria and cells (22).

Biochemical determination of the kinetics of cytochrome *c* oxidase is insufficient to predict the oxygen dependence of mitochondrial or cellular respiration. A synkinetic systems approach is required to explain tissue-specific differences in mitochondrial oxygen affinity, which is a function of the properties of the electron transport pathway (25, 26). The excess capacity of COX ensures that this enzyme operates far from its limiting turnover capacity even at maximum activity of the respiratory chain. When the excess capacity of COX is reduced, then COX is pushed to increasing turnover at identical rates of mitochondrial respiration. As a consequence, the mitochondrial p_{50} declines. Downregulation of cytochrome *c* oxidase activity, therefore, increases the degree of oxyconformance in the low-oxygen range (Figure 1). Reversible inhibition of COX by nanomolar levels of NO induces oxyconformance to a much higher extent (8). An entirely different mechanism for the control of oxyconformance has been proposed by Chandel *et al*. (16), based on reversible downregulation of isolated COX after conditioning at oxygen levels of 15-30 mmHg (2-4 kPa). This putative control of mitochondrial respiration by allosteric changes of COX is unconvincing for two reasons. *(1)* Some hours of conditioning is required for the isolated enzyme, whereas the oxygen effect is instantaneous on embryonic cardiomyocytes (9), and *(2)* owing to the high excess capacity of this enzyme (100 % according to Figure 1; or even 400 % according to data of Budinger *et al*., (9)), over-proportional inhibition of COX is required but was not found to explain downregulation of cellular respiration. In the heart and to a lesser extent in the liver, pathway flux is limited at kinetic oxygen saturation by electron input into COX from the respiratory chain, as expressed by the excess capacity of COX and reflected in a low flux control coefficient (25, 26). Cytochrome *c* oxidase exerts increasing control over respiration at severely limiting oxygen levels <0.1 kPa or <1 mmHg (23).

We were concerned about the potential effect of the time course of oxygen depletion in the closed-chamber respirometer on the respiratory capacity and oxygen kinetics of isolated mitochondria. Changes of mitochondrial protein concentration influence the aerobic-anoxic transition time at any given metabolic state. Using various dilutions of rat liver mitochondria, the transition time between kinetic oxygen saturation at 1.1 kPa (10 mmHg) and anoxia was varied 10-fold in the range of 30 to 300 s, which did not exert any influence on the mitochonrial p_{50} (40). Such kinetic independence was also reported for isolated heart mitochondria (25). Similarly, repeated aerobic-anoxic transitions with intermittent reoxygenations to low oxygen levels did not result in an increase of the p_{50}, when mitochondria were maintained for 2 h at oxygen pressures <2.5 kPa (<20 mmHg). On the contrary, the p_{50} declined moderately as a function of the time-dependent loss of respiratory capacity (Figure 2). Respiratory instability was obtained with time of exposure, even when

mitochondria were maintained continuously above 8 kPa (60 mmHg) oxygen pressure (30 °C), ruling out the possibility that low oxygen or repeated ischemia-reperfusion were responsible for mitochondrial injury (Figure 2). The main mitochondrial defects of long-term exposure were *(1)* cytochrome *c* release (reversed by addition of external cytochrome *c*; Figure 2) which results in increased mitochondrial superoxide production (13), and *(2)* limitation of the phosphorylation system (reversed by uncoupling with FCCP; Figure 2; see also ref. (3)). Mitochondrial respiration is more stable in an improved mitochondrial medium (24). In agreement with a study by Taylor et al. (65), these results do not support the hypotheses that oxyconformance of mitochondrial respiration is caused by conditioning of cytochrome *c* oxidase during exposure to oxygen levels of 2 to 20 mmHg or even up to 50 µM (4 kPa or 30 mmHg (15, 16)).

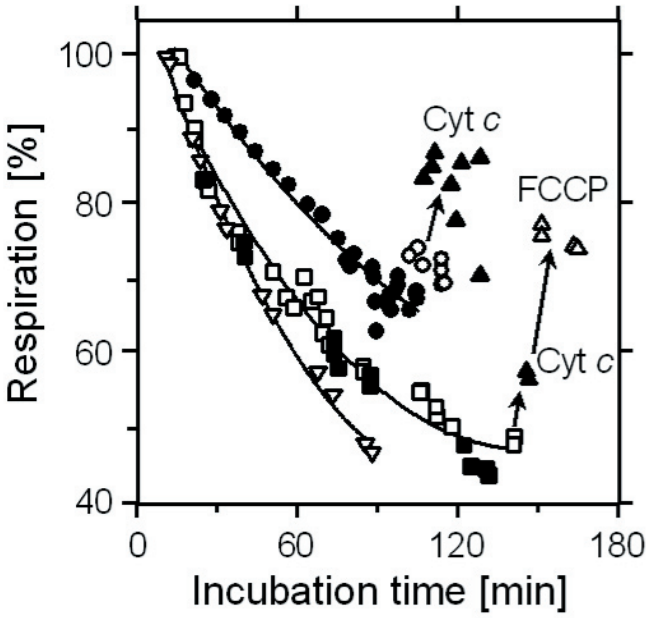

Figure 2. Decline of respiration in isolated rat liver mitochondria as a function of time during incubation in various oxygen regimes: always >80 µM (8 kPa or 60 mmHg; open downward triangles); series of aerobic-anoxic transitions with reoxygenations to high oxygen levels (>25 µM; 2.5 kPa or 20 mmHg; open squares and open circles), or aerobic-anoxic transitions with maximum oxygen levels always maintained <25 µM (closed symbols). Addition of catalase to the medium improved respiratory stability (circles). Oxygen flux is expressed relative to initial respiratory rates. Non-linear fits indicate trends in experiments with identical conditions. Addition of 10 µM cytochrome *c* partly restored respiration. A further increase was obtained after uncoupling by 2 µM FCCP (arrows). The incubation medium MiR03 contained 10 mM succinate, 0.5 µM rotenone, 1 mM ATP, >1 mM ADP, 200 mM sucrose, 20 mM HEPES, 0.5 mM EGTA, 1 g/l BSA, 3 mM $MgCl_2$, 20 mM taurine and 10 mM KH_2PO_4 (pH 7.1; 30 °C; from Lassnig *et al.*, (40)).

BIPHASIC OXYGEN KINETICS: MITOCHONDRIAL AND NON-COX RESPIRATION

Hyperbolic Michaelis-Menten kinetics suggests substrate saturation of flux, theoretically reaching 98 % of maximum at a substrate concentration of 50 times the p_{50} (corresponding to 2 kPa or 15 mmHg at a p_{50} of 0.04 kPa). In many cases, hower, mitochondrial and cellular respiration continues to increase significantly at such high oxygen levels, resulting in biphasic oxygen kinetics (28). Oxygen dependence of respiration in this high-oxygen range up to air saturation has escaped detection in many cases, as illustrated by an experimental example with fibroblasts (33). A continuous decline of oxygen concentration is obtained over time in a closed chamber respirometer (Figure 3A; cO_2). This decline might be approximated by a straight line on a conventional chart recorder trace, which then would imply a constant respiratory flux (the negative slope) and oxygen-independence to very low oxygen levels. Continuous calculation of the time derivative of digitally recorded oxygen concentration, however, clearly reveals an oxygen-dependent attenuation of respiration even at >2 kPa or 20 µM (Figure 3A; JO_2). Cellular oxygen kinetics is hyperbolic when zooming into the low-oxygen range <1 kPa or 10 µM (Figure 3B). A kinetic plot over the full oxygen range illustrates the biphasic oxygen dependence of respiration in human fibroblasts and endothelial cells (Figure 4). This biphasic pattern is not restricted to cells but is observed in isolated mitochondria (28).

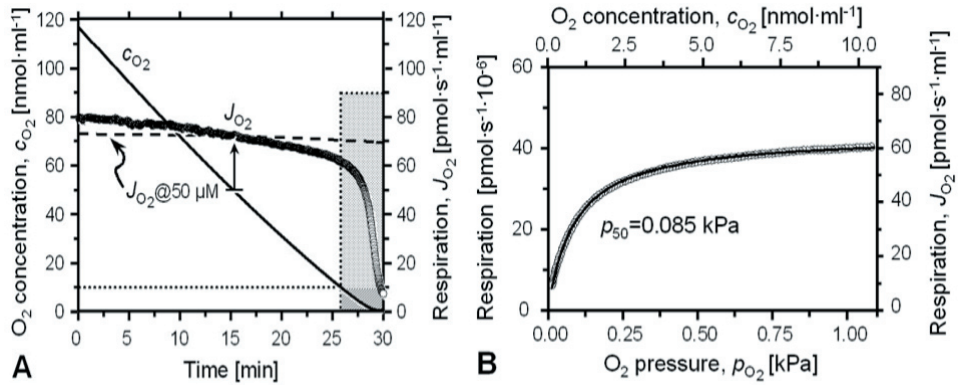

Figure 3. High-resolution respirometry with suspended human foreskin fibroblasts in the Oroboros *Oxygraph-2k*. **A**. Oxygen concentration, cO_2, and respiratory oxygen flux, JO_2, as a function of time in an aerobic-anoxic transition. The significant decline of oxygen flux at high oxygen (circles) was oxygen dependent, whereas loss of respiratory capacity with time (stippled line) contributed to only a small extent. The stippled line shows interpolations of oxygen flux, JO_2, at 50 µM O_2 measured in repeated aerobic-anoxic transitions before and after this section of the experiment. The shaded square indicates the section of the low oxygen range (dashed: concentration; dotted: flux), over a time interval of 3.8 min or 227 s. **B**. Kinetic plot of oxygen flux, JO_2, as a function of oxygen concentration or partial pressure in the low oxygen range. Data points are shown by circles, where flux is calculated at 2-s time intervals with corrections for the exponential response time of the oxygen sensor and the oxygen dependence of instrumental background oxygen flux. Maximum respiration was calculated at 43.4 pmol·s^{-1}·10^{-6} cells, and the oxygen pressure at half-maximum respiration, p_{50} was 0.089 kPa (0.67 mmHg, calculated in the 1.1 kPa range). Modified after Hütter et al. (33).

The oxyconforming component of respiration was calculated as the difference between total cellular respiration (Figure 4A; upper trace) and the hyperbolic component in the low-oxygen range (Figure 3B; extrapolated in Figure 4A; dotted line). This oxyconforming component was proportional to oxygen pressure, although a saturation effect towards air saturation cannot be excluded (Figure 4). After uncoupling by FCCP, respiration was inhibited by rotenone and antimycin A in independent experiments at various levels of oxygen (33). Rotenone and antimycin-A are effective inhibitors of complexes I and III of the respiratory chain and thus inhibit electron transport to cytochrome *c* oxidase. Similar to the oxyconforming component of respiration, the inhibited oxygen uptake of cells (non-COX respiration) increases proportional to oxygen pressure in the experimental range (Figure 4A; circles).

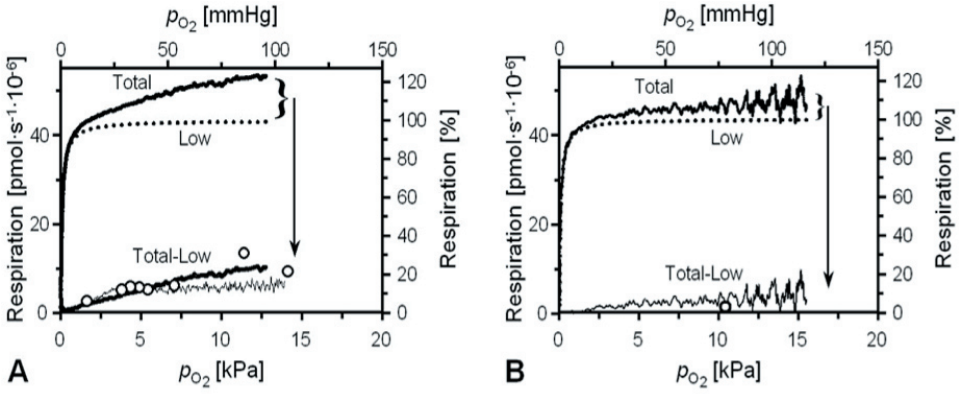

Figure 4. Oxygen dependence of routine respiration (pmol $O_2 \cdot s^{-1} \cdot 10^{-6}$ cells) in culture medium of (**A**) human fibroblasts ($1.5 \cdot 10^6$ cells per ml; from Figure 3; Dulbecco´s modified Eagles´s medium) and (**B**) human umbilical vein endothelial cells (HUVEC; $0.8 \cdot 10^6$ cells per ml; in EGM). Oxygen kinetics is biphasic over the full experimental oxygen range. The dotted line shows the extrapolation of the monophasic hyperbolic relation calculated over the standard low oxygen range (<1.1 kPa) for analysis of mitochondrial oxygen kinetics (Low; A: from Figure 3B; B: maximum respiration of HUVEC was 43.7 pmol·s^{-1}·10^{-6} cells or 34 pmol·s^{-1}·ml^{-1}; p_{50}=0.074 kPa or 0.56 mmHg). At high oxygen, the difference between total cellular respiration (Total) and the extrapolated hyperbolic fit was directly proportional to oxygen pressure (Total-Low; A: solid traces show the difference calculated from two aerobic-anoxic transitions). Open circles show respiration inhibited by rotenone and antimycin A. Modified after Hütter et al. (33) (A) and Gnaiger et al. (28) (B).

80-90 % of the oxygen consumed by an organism is considered to be reduced to water by cytochrome *c* oxidase, the terminal enzyme of the respiratory chain (34, 49, 50). Appart from COX, therefore, a significant potential (10-20 % of total respiration) exists for oxygen utilization by the >100 known oxidoreductases with dioxygen as substrate and by autoxidation of reduced compounds in the cell. Although it is well established that many oxidases, such as xanthine oxidase or monoamino oxidase, have K_m' values for oxygen more than two orders of magnitude higher than COX (68), surprisingly little attention has be paid to the oxygen dependence of non-COX respiration or non-mitochondrial respiration in intact

cells (58). When measured close to air saturation, the non-mitochondrial contribution to organismic respiration is overestimated significantly, owing to the low intracellular oxygen levels in tissues and the strong oxyconformance of non-COX respiration (Figure 4). The conventionally assumed 10 % share to total respiration needs downward correction even under normoxia. Although a quantitatively minor component of total respiration, hypoxic limitation of non-COX oxygen consumption has potentially important consequences on redox signalling (37, 44), biosynthetic reactions with a requirement of molecular oxygen (66), and perhaps on oxidative repair of damaged DNA and RNA (1).

In beef heart submitochondrial particles, hydrogen peroxide and superoxide radical production increase near-linearly with oxygen pressure from 0 to 100 kPa (pure oxygen saturation (6)). ROS production is reduced under hypoxia in pulmonary but not renal artery mitochondria (44). NADH-ubiquinone reductase (complex I) and ubiquinol-cytochrome *c* reductase (complex III) comprise the main sites of electron leak, although in various cell types mitochondrial glycerophosphate dehydrogenase-dependent hydrogen peroxide production represents another effective branch for the electron leak (18). Their common compound ubisemiquinone provides the electrons for mitochondrial non-COX oxygen consumption and ROS production (6),

$$J = pO_2 \cdot (UQH^{\bullet}) \cdot k \qquad (1)$$

The concentration of reduced intermediates potentially reacting with dioxygen, such as ubisemiquinone, ($UQH^{\bullet}$), depends on metabolic state (7) and mitochondrial type (44). In addition, nitric oxide not only inhibits complexes I and IV of the respiratory chain, but regulates mitochondrial production of H_2O_2 (7, 53). In general, therefore, mitochondrial superoxide radical and hydrogen peroxide production are not simple functions of pO_2, which renders reaction (1) an ambiguous or versatile oxygen sensor. Components of the electron transport chain become over-proportionally reduced under conditions of excessive substrate supply and low pO_2. Despite progressive oxygen limitation (Eq. 1), therefore, electron leak and ROS production may increase under hypoxia and reductive stress (17, 42).

In heart mitochondria, rotenone inhibits H_2O_2 production, but subsequent addition of antimycin A restores or even stimulates the rate of hydrogen peroxide generation (6). Importantly, rotenone-inhibited cellular oxygen consumption remains constant after addition of antimycin A (33), which may be taken as indirect evidence for a significant non-COX contribution to rotenone/antimycin A-inhibited respiration in fibroblasts. Even the mitochondrial outer membrane monoamino oxidase activity may surpass hydrogen peroxide production by the inner mitochondrial membrane (7). Consequently, respiration inhibited by antimycin A and particularly by cyanide cannot simply be interpreted as non-mitochondrial respiration. Caution is required since cyanide is not specific for cytochrome *c* oxidase but is a direct inhibitor of other oxidases, such as urate oxidase (56) and inhibits the heme-containing catalase (20). Cyanide inhibition can in fact depress cellular respiration close to zero, particularly after cell membrane permeabilization when the soluble reducing cytosolic components are released and diluted in the mitochondrial incubation medium (48).

A simple kinetic model may explain at least in part the biphasic pattern of respiration observed in small cells with minor intracellular oxygen gradients. The p_{50} measured in the well-mixed incubation medium of these cells is close to the p_{50} of isolated mitochondria

(Figure 1 and Figure 3B (61)). With a lumped apparent K_m' for all non-COX reactions that is 100 times higher than the p_{50} (10 versus 0.1 kPa), total cellular respiration can be simulated in the range of anoxia to air saturation (Figure 5A). Moreover, the oxyconforming non-COX component of respiration is shown to be insignificant in the low-oxygen range used for calculating the hyperbolic fit (Figure 5B). An extension of these studies up to pure oxygen saturation will help elucidating the contribution of non-saturable autoxidation processes to the oxyconformance of cellular respiration. On the other hand, oxygen kinetics of purified COX needs to be studied by high-resolution respirometry to test the hypothesis that the biphasic pattern of oxyconformance is exclusively due to mitochondrial and non-mitochondrial mechanisms of oxygen consumption which are not related to cytochrome *c* oxidase.

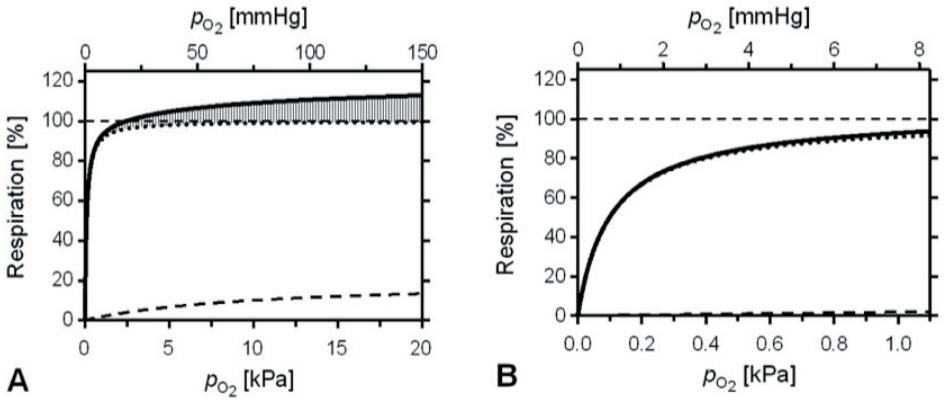

Figure 5. A simple model of biphasic oxygen kinetics in cells, including mitochondrial kinetics with an extracellular p_{50} of 0.1 kPa (0.75 mmHg; dotted lines; maximum oxygen flux at 100 %), and the kinetics of various oxidases with a lumped apparent K_m' of 10 kPa (75 mmHg; assuming these oxidases reach 20 % of mitochondrial respiration at kinetic saturation >100 kPa; dashed lines). Total respiration (full lines) is the sum of the mitochondrial and the oxyconforming non-COX components. **A**: Oxygen range up to air saturation, when the lumped oxidases reach 67 % of their maximum capacity. **B**: Low oxygen range of mitochondrial kinetics, showing that the error is negligable when calculating a hyperbolic fit for total respiration at pO_2<1.1 kPa.

OXYGEN DIFFUSION AND OXYCONFORMANCE

Suspended endothelial cells are spherical with a radius of 5-7 µm, but diffusion distances to mitochondria are reduced owing to the large nucleus which occupies a significant fraction of the central cellular volume (26). Correspondingly, intracellular oxygen gradients are small in endothelial cells (61) and fibroblasts (0.0013 and 0.0028 nL volume per cell, respectively (33)). Routine respiration of endothelial cells is 30 to 40 $pmol \cdot s^{-1} \cdot 10^{-6}$ cells, and is increased 2.5- to 3.5-fold by uncoupling (59, 61). By comparison, rod-shaped adult cardiomyocytes are large (Table 1). Compared to routine respiration in endothelial cells and fibroblasts, activated or uncoupled cardiomyocytes respire at a 50- to

100-fold higher oxygen flow per cell, i.e. 2,000 to 4,000 pmol·s^{-1}·10^{-6} cells ((36, 47, 71) corrected to 37 °C with a Q_{10} of 1.8 (46)). Correspondingly, significant intracellular oxygen gradients (64) give rise to a 10-fold difference between the mitochondrial p_{50} (Figure 1) and extracellular p_{50} values determined in active cardiomyocytes (Figure 6).

Diffusion limitation is further aggravated in permeabilized fiber bundles with a radius of 35 up to 200 μm (38, 52). For comparison, 200 μm away from the nearest blood vessel, the pO_2 drops from 1.9 kPa (14 mmHg) to zero in tumors with relatively low aerobic capacity (30). In permeabilized myocardial fiber bundles the microcirculation is disrupted, myoglobin is released, and the mass-specific respiratory activity is 600 pmol·s^{-1}·mg^{-1} dry weight in the ADP-activated state 3 ((24) measurements converted from 30 °C to 37 °C with a Q_{10} of 1.8; compared to 2,000 pmol·s^{-1}·mg^{-1} dry weight for the maximally active dog heart (46)). Relative to isolated mitochondria, a staggering 100-fold increase of the extracellular p_{50} is measured in heavily stirred permeabilized fiber bundles prepared from rat heart and soleus muscle (39), in which case oxyconformance extends up to air saturation in terms of a monophasic hyperbolic oxygen dependence (Figure 6). Fatigue is accelerated in skeletal muscle fibers of the frog at an oxygen pressure of 4 kPa (30 mmHg (60)) which may fall into the region of initial diffusion limitation (Figure 6B). Similarly, oxygen conformation up to air saturation in superfused frog sartorius muscle is subject to diffusion limitation, although metabolic suppression mediated by signals triggered by a cellular oxygen sensor may always be difficult to exclude (5). Increased diffusion distances are in line with the distinct kinetic responses to external oxygen, when highly oxygen-independent fibroblasts and endothelial cells are compared with oxyconforming cardiomyocytes and fiber bundles (Figs. 4 and 6), spanning a 0.1·10^6-fold volume range (Table 1).

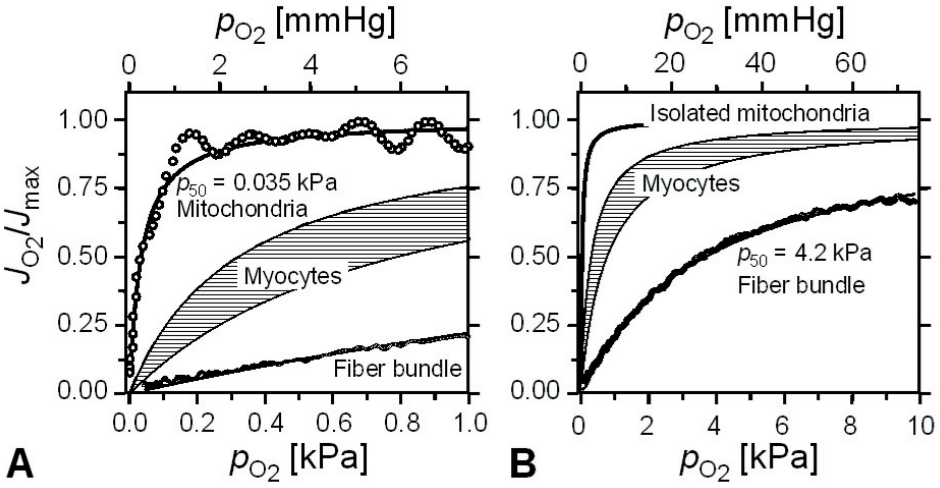

Figure 6. Hyperbolic relation of mitochondrial active respiration, JO_2, and oxygen pressure, pO_2, in isolated heart mitochondria at state 3 (stimulated by ADP; after Gnaiger et al. (25)); isolated cardiomyocytes (resting (36) and stimulated by uncoupling (51)) and permeabilized rat skeletal muscle fibers (M. soleus) at state 3 (stimulated by ADP; after Kuznetsov et al. (39)). **A** and **B** show different ranges of oxygen pressure.

Table 1. Schematic geometry of cell systems with increasing oxygen diffusion limitation and oxyconformance, expressed as Δp_{50}, the difference between extracellular and mitochondrial p_{50}.

Cell	Shape	Radius	Length	Volume	Δp_{50}	
		µm	mm	nL	kPa	mmHg
Endothelial cell	Spherical	6.8	0.014[#]	0.0013	0.01[†]	0.1
Cardiomyocyte	Cylindrical	10	0.1	0.03	0.3-0.8[‡]	2-6
Fiber bundle	Intertwined	150	2	140	1.4-6.8[§]	10-50

[#] Diameter and radius of suspended human umbilical vein endothelial cells (26), calculated according to measured volume (33).
[†] From ref. (61).
[‡] Radius and length from ref. (35); range of Δp_{50} from ref. (36, 51).
[§] Radius and length from ref. (52); fiber bundels are intertwined in the stirred respirometer chamber; range of Δp_{50} is the mean ± SD from ref. (39).

HYPOXIA AND DOWNREGULATION OF ENERGY DEMAND

Matching of energy demand with energy supply is the prerequisite for homeostatic control of the cellular energy state. Respiration of adult cardiomyocytes becomes diffusion limited below pO_2 values of c. 2 kPa (Figure 7A). Hence induction of anoxic tolerance in cultured adult rat cardiac myocytes by conditioning at 1 % O_2 (1 kPa) (57) is possibly mediated by its effect on mitochondrial function. Hypoxia is partly compensated by increased glycolytic ATP production and accompanied by reversible downregulation of contractile activity (62, 63). An entirely different response is observed in chick embryonic cardiomyocytes (9), which have a 100-fold lower oxygen consumption per cell compared to adult rat cardiomyocytes, and present a much higher degree of oxyconformance which is unrelated to diffusion restriction (Figure 7B). Vertrebrate and particularly bird embryo hearts develop normally in a low-oxygen microenvironment and display low oxidative metabolism. Vascularization and myoglobin are absent in early developmental stages when cardiac function is less oxygen dependent and anoxic tolerance is relatively high (55). Experimental conditions well below air saturation (Figure 7B), therefore, mark the transition from hyperoxia to hypoxia. It remains to be defined, how low the pO_2 needs to be set in the incubation medium to provide a "normoxic" environment for embryonic cardiomyocytes.

The respiratory response of beating embryonic (9) and resting neonatal cardiac cells (11) is immediate, and thus independent of hypoxic conditioning (Figure 7B). It is tempting to interpret the onset of microxic regulation (21) of the neonatal cardiomyocytes (Figure 7B; arrow) as somewhat intermediate between the oxygen response pattern of embryonic and adult heart cells. The proton permeability in neonatal mitochondria is higher than in adult cardiac mitochondria (67). Importantly, at least part of the oxyconformance in neonatal cardiomyocytes is caused by suppression at low oxygen of the proton leak component of oxygen consumption not coupled to ATP synthesis (12). In addition to the inhibition of non-COX respiration (Figure 5), this contributes to an increased biochemical efficiency of ATP production per unit oxygen consumed at low oxygen levels, as supported by studies on isolated mitochondria (27).

Rather than generalizing pO_2-dependent downregulation of respiration and ATP utilization, the striking differences in various developmental stages of cardiac cells warrant explanation. Discussing these different physiological responses to oxygen pressure in cardiomyocytes from mammals and birds at different developmental stages under the umbrella of short-term "hibernation" (10-12, 57, 63) draws attention to the importance of homeostatic control of ATP demand in the face of changes in supply. The adaptive mechanisms of metabolic downregulation in hypometabolic states of hypoxia (31), however, are more clearly appreciated by relating physiological and biochemical control mechanisms to the diversity of oxygen regimes and metabolic challenges met by various types of mitochondria, cells, tissues and organisms.

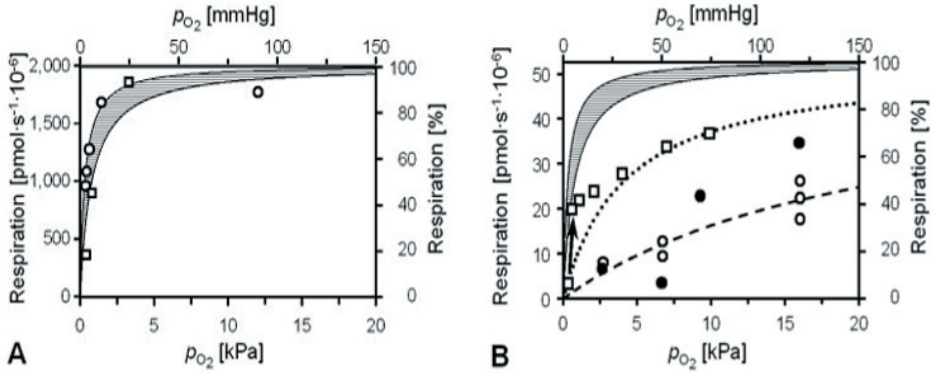

Figure 7. Oxygen dependence of respiration in adult (A) and neonatal or embryonic cardiomyocytes (B). **A**. Circles and squares: data from Stumpe and Schrader (62, 63); activated cardiomyocytes in an oxystat system (left *Y*-axis; based on 4 mg protein per 10^6 cells (57, 71)). The small degree of apparent oxyconformance is within the range of cellular diffusion limitation. **B**. Squares: resting neonatal rat cardiomyocytes; data from Casey and Arthur (11); strongly biphasic (arrow), in contrast with a hyperbolic oxygen dependence (dotted line; permeabilized myocardial fiber bundles with p_{50} of 4.2 kPa; right *Y*-axis). Circles: acute or prolonged (open) and sustained (closed) exposure to various oxygen levels in beating chick embryo cardiomyocytes; data from Budinger et al. (9) (dashed line: hyperbolic trend line for open circles with apparent p_{50}>20 kPa). Adult cardiomyocyte oxygen kinetics is shown as a common reference in both panels as the hatched area, lower boundary line: p_{50} of 0.32 kPa (2.4 mmHg (36), upper boundary line: 0.79 kPa (5.9 mmHg (51)) for resting and uncoupled cardiomyocytes (right *Y*-axes).

REFERENCES

1. Aas PA, Otterlei M, Falnes PO, Vagbo CB, Skorpen F, Akbari M, Sundheim O, Bjoras M, Slupphaug G, Seeberg E, and Krokan HE. Human and bacterial oxidative demethylases repair alkylation damage in both RNA and DNA. *Nature* 421: 859-863, 2003.
2. Arthur PG, Giles JJ, and Wakeford CM. Protein synthesis during oxygen conformance and severe hypoxia in the mouse muscle cell line C_2C_{12}. *Biochim Biophys Acta* 1475: 83-89, 2000.
3. Aw TY, Anderssen BS, and Jones DP. Suppression of mitochondrial respiratory function after

short-term anoxia. *Am J Physiol* 252: C362-C368, 1987.
4. Bernardi P, Petronilli V, Di Lisa F, and Forte M. A mitochondrial perspective on cell death. *Trends Biochem Sci* 26: 112-117, 2001.
5. Boutilier RG, and St-Pierre J. Adaptive plasticity of skeletal muscle energetics in hibernating frogs: mitochondrial proton leak during metabolic depression. *J Exp Biol* 205: 2287-2296, 2002.
6. Boveris A. Mitochondrial production of superoxide radical and hydrogen peroxide. In: Reivich, M., Coburn, R., Lahiri, S., Chance, B. (Eds.). *Tissue Hypoxia and Ischemia*. Thieme, Stuttgart, pp. 67-82, 1977.
7. Boveris A, and Cadenas E. Mitochondrial production of hydrogen peroxide. Regulation by nitric oxide and the role of ubisemiquinone. *Life* 50: 245-250, 2000.
8. Brown G. Regulation of mitochondrial respiration by nitric oxide inhibition of cytochrome *c* oxidase. *Biochim Biophys Acta* 1504: 46-57, 2001.
9. Budinger GRS, Chandel N, Shao ZH, Li CQ, Melmed A, Becker LB, and Schumacker PT. Cellular energy utilization and supply during hypoxia in embryonic cardiac myocytes. *Am J Physiol* 270: L44-L53, 1996.
10. Budinger GRS, Duranteau J, Chandel N, and Schumacker PT. Hibernation during hypoxia in cardiomyocytes. Role of mitochondria as the O_2 sensor. *J Biol Chem* 273: 3320-3326, 1998.
11. Casey TM, and Arthur PG. Hibernation in noncontracting mammalian cardiomyocytes. *Circulation* 102: 3124-3129, 2000.
12. Casey TM, Pakay JL, Guppy M, and Arthur PG. Hypoxia causes downregulation of protein and RNA synthesis in noncontracting mammalian cardiomyocytes. *Circ Res* 90: 777-783, 2002.
13. Cai J, and Jones DP. Superoxide in apoptosis. *J Biol Chem* 273: 11401-11404, 1998.
14. Chandel NS, Budinger GRS, Choe SH, and Schumacker PT. Cellular respiration during hypoxia. Role of cytochrome oxidase as the oxygen sensor in hepatocytes. *J Biol Chem* 272: 18808-18816, 1997.
15. Chandel N, Budinger GRS, Kemp RA, and Schumacker PT. Inhibition of cytochrome-*c* oxidase activity during prolonged hypoxia. *Am J Physiol* 268: L918-L925, 1995.
16. Chandel NS, Budinger GRS, and Schumacker PT. Molecular oxygen modulates cytochrome *c* oxidase function. *J Biol Chem* 271: 18672-18677, 1996.
17. Chandel NS; and Schumacker PT. Cellular oxygen sensing by mitochondria: old questions, new insight. *J Appl Physiol* 88: 1880-1889, 2000.
18. Drahota Z, Chowdhury SKR, Floryk D, Mrácek T, Wilhelm J, Rauchova H, Lenaz G, and Houstek J. Glycerophosphate-dependent hydrogen peroxide production by brown adipose tissue mitochondria and its activation by ferricyanide. *J Bioenerg Biomembr* 34: 105-113, 2002.
19. Erecinska M, and Silver IA. Tissue oxygen tension and brain sensitivity to hypoxia. *Respir Physiol* 128: 263-276, 2001.
20. Fridovich I. Oxygen toxicity: a radical explanation. *J Exp Biol* 201: 1203-1209, 1998.
21. Gnaiger E. Homeostatic and microxic regulation of respiration in transitions to anaerobic metabolism. In: Bicudo J.E.P.W. (ed.) *The vertebrate gas transport cascade: Adaptations to environment and mode of life.* CRC Press, Boca Raton, Ann Arbor, London, Tokyo: 358-370, 1993.
22. Gnaiger E. Bioenergetics at low oxygen: dependence of respiration and phosphorylation on oxygen and adenosine diphosphate supply. *Respir Physiol* 128: 277-297, 2001.
23. Gnaiger E, and Kuznetsov AV. Mitochondrial respiration at low levels of oxygen and cytochrome *c*. *Biochem Soc Trans* 30: 252-258, 2002.
24. Gnaiger E, Kuznetsov AV, Schneeberger S, Seiler R, Brandacher G, Steurer W, and Margreiter R. Mitochondria in the cold. In: Heldmaier G., Klingenspor M. (eds) *Life in the Cold*. Heiderlberg, Berlin, New York: Springer, 2000, pp. 431-442
25. Gnaiger E, Lassnig B, Kuznetsov AV, and Margreiter R. Mitochondrial respiration in the low

oxygen environment of the cell: Effect of ADP on oxygen kinetics. *Biochim Biophys Acta* 1365: 249-254, 1998.

26. Gnaiger E, Lassnig B, Kuznetsov AV, Rieger G, and Margreiter R. Mitochondrial oxygen affinity, respiratory flux control, and excess capacity of cytochrome *c* oxidase. *J Exp Biol* 201: 1129-1139, 1998.
27. Gnaiger E, Méndez G, and Hand SC. High phosphorylation efficiency and depression of uncoupled respiration in mitochondria under hypoxia. *Proc Natl Acad Sci USA* 97: 11080-11085, 2000.
28. Gnaiger E, Steinlechner R, Méndez G, Eberl T, and Margreiter R. Control of mitochondrial and cellular respiration by oxygen. *J Bioenerg Biomembr* 27: 583-596, 1995.
29. Heerlein K, Schulze A, Bärtsch P, and Mairbäurl H. Hypoxia reduces cellular oxygen consumption and Na/K-ATPase activity of alveolar epithelial cells. *High Altitude Med. Biol.* 3: 449, 2002.
30. Helmlinger G, Yuan F, Dellian M, and Jain RK. Interstitial pH and pO_2 gradients in solid tumors *in vivo*: High-resolution measurements reveal a lack of correlation. *Nature Medicine* 3: 177-182, 1997.
31. Hochachka PW, Buck LT, Doll CJ, and Land SC. Unifying theory of hypoxia tolerance: Molecular/metabolic defense and rescue mechanisms for surviving oxygen lack. *Proc Natl Acad Sci USA* 93: 9493-9498, 1996.
32. Hochachka PW, Lutz PL, Sick T, Rosenthal M, and Van den Thillart G. (eds) *Surviving Hypoxia: Mechanisms of Control and Adaptation*. Boca Raton, Ann Arbor, London, Tokyo: CRC Press, 1993.
33. Hütter E, Renner K, Jansen-Dürr P, and Gnaiger E. Biphasic oxygen kinetics of cellular respiration and linear oxygen dependence of antimycin A inhibited oxygen consumption. *Molec Biol Rep* 29: 83-87, 2002.
34. Jackson MJ, Papa S, Bolanos J, Bruckdorfer R, Carlsen H, Elliott RM, Flier J, Griffiths HR, Heales S, Holst B, Lorusso M, Lund E, Moskaug JO, Moser U, Di Paola M, Polidori MC, Signorile A, Stahl W, Vina-Ribes J, and Astley SB. Antioxidants, reactive oxygen and nitrogen species, gene induction and mitochondrial function. *Molec Aspects Med* 23: 209-285, 2002.
35. Jones DP, and Kennedy FG. Analysis of intracellular oxygenation of isolated adult cardiac myocytes. *Am J Physiol* 250: C384-C390, 1986.
36. Kennedy FG, and Jones DP. Oxygen dependence of mitochondrial function in isolated rat cardiac myocytes. *Am J Physiol* 250: C374-C383, 1986.
37. Kietzmann T, Fandrey J, and Acker H. Oxygen radicals as messengers in oxygen-dependent gene expression. *News Physiol Sci* 15: 202-208, 2000.
38. Kongas O, Yuen TL, Wagner MJ, van Beek JHGM, and Krab K. High K_m of oxidative phosphorylation for ADP in skinned muscle fibers: where does it stem from? *Am J Physiol* 283: C743-C751, 2002.
39. Kuznetsov AV, Lassnig B, Margreiter R, and Gnaiger E. Diffusion limitation of oxygen versus ADP in permeabilized muscle fibers. In: Larsson C., Påhlman I.-L., Gustafsson L. (eds) *BioThermoKinetics in the Post Genomic Era*. Göteborg: Chalmers Reproservice, 1998, p.273-276,
40. Lassnig B, Kuznetsov AV, Margreiter R, and Gnaiger E. Aerobic-anoxic transitions and regulation of mitochondrial oxygen flux. In: Larsson C., Påhlman I.-L., Gustafsson L. (eds) *BioThermoKinetics in the Post Genomic Era*. Göteborg: Chalmers Reproservice, 1998, p.312-316,
41. Lefebvre VHL, Steenbrugge MV, Beckers V, Roberfroid M, and Buc-Calderon VHL. Adenine nucleotides and inhibition of protein synthesis in isolated hepatocytes incubated under different pO_2 levels. *Arch Biochem Biophys* 304: 322-331, 1993.
42. Lemasters JJ, and Nieminen A-L. Mitochondrial oxygen radical formation during reductive and oxidative stress to intact hepatocytes. *Biosci Rep* 17: 281-291, 1997.

43. Metzen E, Wolff M, Fandrey J, and Jelkmann W. Pericellular pO_2 and O_2 consumption in monolayer cultures. *Respir Physiol* 100: 101-106, 1995.
44. Michelakis ED, Hampl V, Nsair A, Wu X, Harry G, Haromy A, Gurtu R, and Archer SL. Diversity in mitochondrial function explains differences in vascular oxygen sensing. *Circ Res* 90: 1307-1315, 2002.
45. Miller WM, Wilke CR, and Blanch HW. Effects of dissolved oxygen concentration on hybridoma growth and metabolism in continuous culture. *J Cell Physiol* 132: 524-530, 1987.
46. Mootha VK, Arai AE, and Balaban RS. Maximum oxidative phosphorylation capacity of the mammalian heart. *Am J Physiol* 272: H769-H775, 1997.
47. Noll T, Koop A, and Piper HM. Mitochondrial ATP-synthase activity in cardiomyocytes after aerobic-anaerobic metabolic transitions. *Am J Physiol* 262: C1297-C1303, 1992.
48. Renner K, Kofler R, and Gnaiger E. Mitochondrial function in glucocorticoid triggered T-ALL cells with transgenic Bcl-2 expression. *Molec Biol Rep* 29: 97-101, 2002.
49. Rich P. Chemiosmotic coupling: The cost of living. *Nature* 241: 583, 2003.
50. Rolfe DFS, and Brown GC. Cellular energy utilization and molecular origin of standard metabolic rate in mammals. *Physiol Rev* 77: 731-758, 1997.
51. Rumsey WL, Schlosser C, Nuutinen EM, Robiolio M, and Wilson DF. Cellular energetics and the oxygen dependence of respiration in cardiac myocytes isolated from adult rat. *J Biol Chem* 265: 15392-15402, 1990.
52. Saks VA, Belikova YO, and Kuznetsov AV. In vivo regulation of mitochondrial respiration in cardiomyocytes: specific restrictions for intracellular diffusion of ADP. *Biochim Biophys Acta* 1074: 302-311, 1991.
53. Sarkela TM, Berthiaume J, Elfering S, Gybina AA, and Giulivi C. The modulation of oxygen radical production by nitric oxide in mitochondria. *J Biol Chem* 276: 6945-6949, 2001.
54. Schumacker PT, Chandel N, and Agusti AGN. Oxygen conformance of cellular respiration in hepatocytes. *Am J Physiol* 265: L395-L402, 1993.
55. Sedmera D, Kucera P, and Raddatz E. Developmental changes in cardiac recovery from anoxia-reoxygenation. *Am J Physiol* 283: R379-R388, 2002.
56. Sies H. Oxygen gradients during hypoxic steady states in liver. *Hoppe Seylers Z Physiol Chem* 358: 1021-1032, 1977.
57. Silverman HS, Wei S-K, Haigney MCP, Ocampo CJ, and Stern MD. Myocyte adaptation to chronic hypoxia and development of tolerance to subsequent acute severe hypoxia. *Circ Res* 80: 699-707, 1997.
58. Skulachev VP. Role of uncoupled and non-coupled oxidations in maintenance of safely low levels of oxygen and its one-electron reductants. *Quart Rev Biophys* 29: 169-202, 1996.
59. Stadlmann S, Rieger G, Amberger A, Kuznetsov AV, Margreiter R, and Gnaiger E. H_2O_2-mediated oxidative stress versus cold ischemia-reperfusion: mitochondrial respiratory defects in cultured human endothelial cells. *Transplantation* 74: 1800-1803, 2002.
60. Stary CM, and Hogan MC. Effect of varied extracellular pO_2 on muscle performance in *Xenopus* single skeletal muscle fibers. *J Appl Physiol* 86: 1812-1816, 1999.
61. Steinlechner-Maran R, Eberl T, Kunc M, Margreiter R, and Gnaiger E. Oxygen dependence of respiration in coupled and uncoupled endothelial cells. *Am J Physiol* 271: C2053-C2061, 1996.
62. Stumpe T, and Schrader J. Phosphorylation potential, adenosine formation, and critical pO_2 in stimulated rat cardiomyocytes. *Am J Physiol* 273: H756-H766, 1997.
63. Stumpe T, and Schrader J. Short-term hibernation in adult cardiomyocytes is pO_2 dependent and Ca^{2+} mediated. *Am J Physiol* 280: H42-H50, 2001.
64. Takahashi E, Endoh H, and Doi K. Visualization of myoglobin-facilitated mitochondrial O_2 delivery in a single isolated cardiomyocyte. *Biophys J* 78: 3252–3259, 2000.
65. Taylor DE, Kantrow SP, and Piantadosi CA. Mitochondrial respiration after sepsis and prolonged hypoxia. *Am J Physiol* 275: L139-L144, 1998.

66. Taylor WG, and Camalier RF. Modulation of epithelial cell proliferation in culture by dissolved oxygen. *J Cell Physiol* 111: 21-27, 1982
67. Tiivel T, Kadaya L, Kuznetsov A, Kaambre T, Peet N, Sikk P, Braun U, Ventura-Clapier R, Saks V, Seppet EK. Developmental changes in regulation of mitochondrial respiration by ADP and creatine in rat heart in vivo. *Mol Cell Biochem* 208: 119-28, 2000.
68. Vanderkooi JM, Erecinska M, and Silver IA. Oxygen in mammalien tissue: methods of measurement and affinities of various reactions. *Am J Physiol* 260: C1131-C1150, 1991.
69. Verkhovsky MI, Morgan JE, Puustinen A., and Wikström M. Kinetic trapping of oxygen in cell respiration. *Nature* 380: 268-270, 1996.
70. Wikström M, and Verkhovsky MI. Proton translocation by cytochrome *c* oxidase in different phases of the catalytic cycle. *Biochim Biophys Acta* 1555: 128-132, 2002.
71. Wittenberg BA., and Wittenberg JB. Oxygen pressure gradients in isolated cardiac myocytes. *J Biol Chem* 260: 6548-6554, 1985.